Current Biology 23, 430–435, March 4, 2013 ©2013 Elsevier Ltd All rights reserved http://dx.doi.org/10.1016/j.cub.2013.01.064

Report

Cellular Mechanotransduction Relies on Tension-Induced and Chaperone-Assisted Autophagy

Anna Ulbricht,[1] Felix J. Eppler,[2,7] Victor E. Tapia,[3,7] Peter F.M. van der Ven,[1,7] Nico Hampe,[4] Nils Hersch,[4] Padmanabhan Vakeel,[1,8] Daniela Stadel,[5] Albert Haas,[1] Paul Saftig,[6] Christian Behrends,[5] Dieter O. Fürst,[1] Rudolf Volkmer,[3] Bernd Hoffmann,[4] Waldemar Kolanus,[2] and Jörg Höhfeld[1,*]

[1]Institute for Cell Biology, University of Bonn, Ulrich-Haberland-Str. 61a, 53121 Bonn, Germany
[2]Life and Medical Sciences Institute, University of Bonn, Carl-Troll-Str. 31, 53115 Bonn, Germany
[3]Department of Medicinal Immunology, Charité - University Medicine Berlin, Augustenburger Platz 1, 13353 Berlin, Germany
[4]Institute of Complex Systems 7, Biomechanics, Forschungszentrum Jülich, 52425 Jülich, Germany
[5]Institute of Biochemistry II, Goethe University Medical School, University Hospital Building 74/75, Theodor-Stern-Kai 7, 60528 Frankfurt am Main, Germany
[6]Biochemical Institute, University of Kiel, Olshausenstr. 40, 24098 Kiel, Germany

Summary

Mechanical tension is an ever-present physiological stimulus essential for the development and homeostasis of locomotory, cardiovascular, respiratory, and urogenital systems [1, 2]. Tension sensing contributes to stem cell differentiation, immune cell recruitment, and tumorigenesis [3, 4]. Yet, how mechanical signals are transduced inside cells remains poorly understood. Here, we identify chaperone-assisted selective autophagy (CASA) as a tension-induced autophagy pathway essential for mechanotransduction in muscle and immune cells. The CASA complex, comprised of the molecular chaperones Hsc70 and HspB8 and the cochaperone BAG3, senses the mechanical unfolding of the actin-crosslinking protein filamin. Together with the chaperone-associated ubiquitin ligase CHIP, the complex initiates the ubiquitin-dependent autophagic sorting of damaged filamin to lysosomes for degradation. Autophagosome formation during CASA depends on an interaction of BAG3 with synaptopodin-2 (SYNPO2). This interaction is mediated by the BAG3 WW domain and facilitates cooperation with an autophagosome membrane fusion complex. BAG3 also utilizes its WW domain to engage in YAP/TAZ signaling. Via this pathway, BAG3 stimulates filamin transcription to maintain actin anchoring and crosslinking under mechanical tension. By integrating tension sensing, autophagosome formation, and transcription regulation during mechanotransduction, the CASA machinery ensures tissue homeostasis and regulates fundamental cellular processes such as adhesion, migration, and proliferation.

[7]These authors contributed equally to this work
[8]Present address: Division of Developmental Biology, Department of Pediatrics, Medical College of Wisconsin, Milwaukee, WI 53226, USA
*Correspondence: hoehfeld@uni-bonn.de

Results and Discussion

The CASA-inducing cochaperone BAG3 contains a WW domain at its amino terminus [5] (Figure 1A). Such domains are known to interact with proline-rich motifs [6, 7]. To identify BAG3 interactors, we incubated a peptide array displaying 2296 proline-rich peptides from the human proteome with the BAG3 WW domain. The approach revealed preferential binding of the domain to PPPY and PPSY motifs and led to the identification of the known BAG3 interactor RAPGEF6 [8] and 72 putative novel binding partners (Figures 1A and 1B). Among the latter was synaptopodin-2 (SYNPO2, myopodin), a cytoskeleton adaptor protein that acts as a tumor suppressor in bladder and prostate (Figure 1C) [9–11]. In striated muscles, SYNPO2 localizes together with BAG3 and the actin-crosslinking proteins α-actinin and filamin at Z disks, which are actin-anchoring structures that rely on CASA for their maintenance under mechanical tension [5, 10]. In smooth muscle cells, these proteins colocalize along actin stress fibers that form when tension is generated inside cells during adhesion and migration (Figure S1A, available online). Muscle cells express at least four different SYNPO2 isoforms, SYNPO2a to SYNPO2d, which all contain the PPPY motif recognized by the BAG3 WW domain (Figures 1D and 1E). Binding studies confirmed a WW-PPPY-mediated interaction between BAG3 and SYNPO2 (Figures S1C–S1F). Moreover, BAG3 was readily detectable in immunoprecipitated SYNPO2 complexes, which also contained the CASA chaperone Hsc70, the CASA-mediating ubiquitin adaptor p62, and the CASA client and known SYNPO2 interactor filamin [5, 10] (Figure 1F).

The observed interaction prompted us to investigate whether SYNPO2 is degraded by CASA. Autophagy inhibition by bafilomycin A1 (BafA1) and proteasome inhibition by MG132, known to induce autophagy [12], did not affect the short isoform SYNPO2d, which lacks the amino-terminal PDZ domain (Figures S2A and S2B). Yet, cellular levels of the PDZ-containing isoforms SYNPO2a to SYNPO2c decreased after induction of autophagy and increased upon autophagy inhibition (Figures S2A–S2E). Furthermore, depletion of the autophagy factors ATG5 and ATG7 or of the CASA-inducing cochaperones BAG3 and CHIP stabilized SYNPO2a to SYNPO2c (Figures S2F–S2K). SYNPO2 is apparently degraded by CASA in a PDZ domain-dependent manner.

Degradation may reflect recognition as a chaperone client or a functional involvement of SYNPO2 isoforms in CASA, leading to codegradation during autophagic flux. Notably, SYNPO2 and the CASA client filamin were differently affected by impaired autophagosome-lysosome fusion in mice deficient for the lysosome membrane protein LAMP2 [13]. Filamin forms large proteinaceous aggregates in muscles of these mice [5]. In contrast, SYNPO2 was released from actin-crosslinking structures, i.e., stress fibers in smooth muscle cells and Z disks in soleus muscles, and accumulated in small aggregates and autophagosomes (Figures S2L–S2N). To elucidate a functional involvement in CASA, we treated adherent smooth muscle cells with SYNPO2 siRNAs. This led to a significant depletion of the unstable isoforms SYNPO2a to SYNPO2c but did not reduce SYNPO2d expression (Figure 2A). Notably,

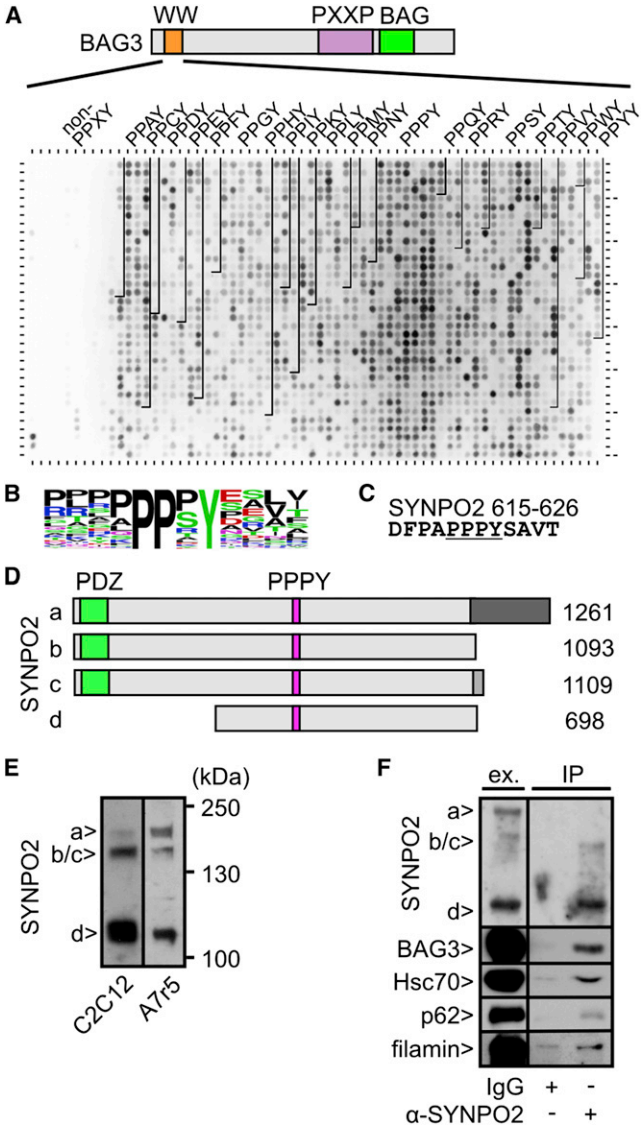

Figure 1. BAG3 Associates with SYNPO2

(A) A peptide array containing 2296 polyproline peptides (12-mers) from ~1750 protein IDs of the human proteome was incubated with the biotin-labeled BAG3 WW domain (aa 20–54), followed by detection of the bound domain. BAG, Hsc70-binding BAG domain.

(B) Amino acid probabilities within the BAG3 WW domain-associated 12-mer peptides.

(C) BAG3 interacts with a PPPY-containing peptide (aa 615–626) of SYNPO2.

(D) Schematic representation of SYNPO2 isoforms expressed in human cells.

(E) Immunodetection of SYNPO2 isoforms in extracts of mouse striated muscle cells (differentiated C2C12) and rat smooth muscle cells (A7r5). SYNPO2b and SYNPO2c cannot be distinguished because of their similar molecular mass (60 μg of protein per lane).

(F) Immunoprecipitation (IP) of SYNPO2 isoforms from A7r5 cells. Isolated complexes were probed for the presence of associated components by immunoblotting with corresponding antibodies. Ex., extract (60 μg of protein per lane)

See Figure S1 for related data.

depletion caused a stabilization of LC3B-II (lipidated LC3B), a marker for autophagosome precursor membranes (phagophores) and autophagosomes [14] (Figures S2O and S2P). SYNPO2a to SYNPO2c thus exert an essential function during

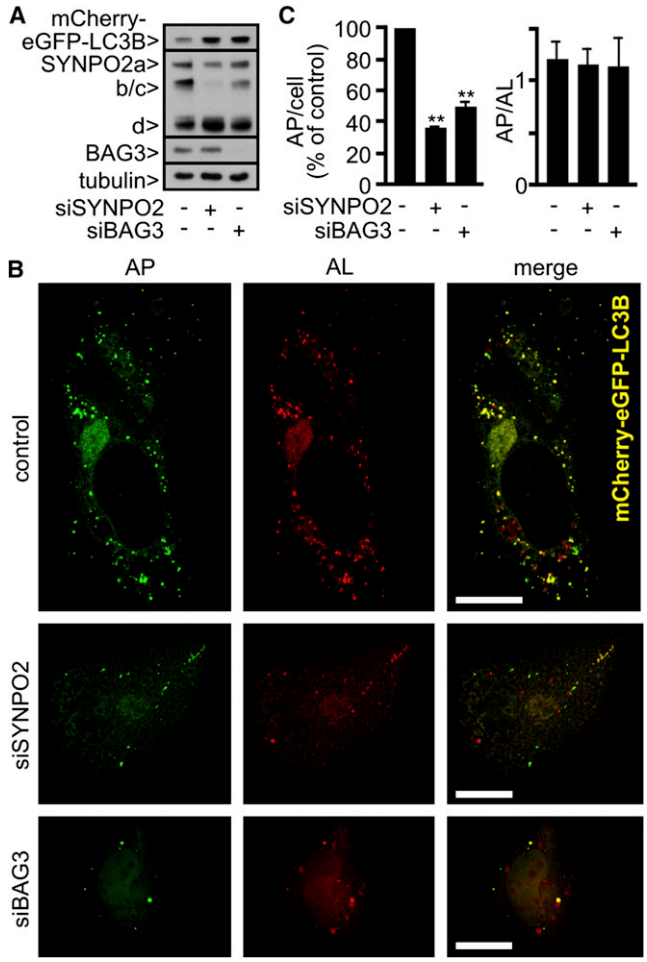

Figure 2. SYNPO2 Is Essential for Autophagosome Formation

(A) A7r5 cells were transfected with a plasmid encoding mCherry-eGFP-LC3B and with control (–), *synpo2*-, or *bag3*-targeting siRNA for 72 hr as indicated, followed by lysis. Extracts were probed with antibodies against the indicated components (60 μg of protein per lane).

(B) Autophagosome (AP, yellow signal in the merge) and autolysosome (AL, red signal in the merge) formation was monitored in adherent A7r5 cells expressing mCherry-eGFP-LC3B. Where indicated, SYNPO2 or BAG3 was depleted by transfection of corresponding siRNAs for 72 hr before fixation. Scale bars represent 20 μm.

(C) Quantification of data obtained as described under (B). Autophagosome number in control cells was set to 100%. The AP/AL ratio was determined by dividing numbers of autophagosomes and autolysosomes per cell. Mean ± SEM, n = 3, 20 cells counted for each sample in each individual experiment, **$p < 0.005$.

See Figure S2 for related data.

autophagy after phagophore formation. Consequences for autophagosome (AP) and (auto)lysosome (AL) formation were analyzed using an mCherry-eGFP-LC3B reporter, which gives rise to yellow fluorescence in autophagosomes and turns red in acidic autolysosomes because of eGFP quenching. Depletion of SYNPO2a to SYNPO2c resulted in a 60%–70% decrease in autophagosome formation, similar to findings for BAG3, whereas autophagosome-lysosome fusion remained unaffected (Figures 2B and 2C). Autophagosome formation during CASA apparently depends on PDZ-containing SYNPO2 isoforms.

The SYNPO2 PDZ domain interacted in a yeast two-hybrid screen with the vacuolar protein sorting 18 homolog (VPS18)

(Figure 3A). VPS18 is a core component of different membrane-tethering complexes, such as the homotypic fusion and vacuole protein sorting (HOPS) complex, which contains, in addition to core components, the RAB7-binding proteins VPS39 and VPS41 to facilitate fusion with lysosomes [15–17]. VPS18 and also the core protein VPS16 coprecipitated with SYNPO2 upon immunoprecipitation from smooth muscle cells, whereas HOPS-specific components did not (Figure 3B). SYNPO2 apparently interacts with a membrane-tethering complex that is distinct from HOPS, in agreement with a role in autophagosome formation but not autophagosome-lysosome fusion (see Figure 2). SYNPO2 immunocomplexes also contained ATG16L1, which is present on preautophagosomal structures (PAS) and phagophores, the phagophore and autophagosome marker LC3B, and the phagophore fusion-factor syntaxin7 [14, 18] (Figure 3B). This further supports a function of the SYNPO2-associated VPS16- and VPS18-containing tethering complex in autophagosome formation. Increased expression of VPS18, previously shown to disrupt membrane fusion [19, 20], and depletion of VPS16 indeed attenuated the degradation of SYNPO2 and the CASA client filamin, respectively (Figures 3C–3F). Finally, VPS16 was also detectable in association with BAG3, but interaction was abrogated by SYNPO2 depletion (Figure 3G). SYNPO2 apparently links the client-processing CASA chaperone machinery to a membrane-tethering and fusion complex that provides autophagosome membranes (Figure 4A).

WW domains and PPxY motifs are interaction modules frequently used in signaling proteins [6, 7]. Among them are the transcriptional coactivators YAP and TAZ (WW domains) and the YAP/TAZ inhibitors LATS1/2 and AMOTL1/2 (PPxY motifs) (Figure 4A). Remarkably, YAP and TAZ are activated under mechanical tension to induce the expression of proteins involved in cell adhesion, including the connective tissue growth factor (CTGF) and filamin [21] (Figure 4B). Activation can be blocked by cytoplasmic retention of YAP/TAZ through binding to LATS1/2, AMOTL1/2, and 14-3-3 proteins (Figure 4A) [6]. Intriguingly, the YAP/TAZ inhibitors LATS1, AMOTL1, and AMOTL2 were all detected as BAG3 WW interactors on the peptide array (Figure 4C). BAG3 might use its WW domain for binding PPxY-containing YAP/TAZ inhibitors and thereby activate YAP/TAZ (Figure 4A). Indeed, BAG3 was found associated with LATS1 and AMOTL1, and BAG3 depletion attenuated YAP/TAZ target gene expression (Figures 4D and 4E). On the other hand, SYNPO2 depletion, which relieves BAG3 from recruitment to the autophagy machinery (see Figure 3G), induced target gene expression (Figure 4F). BAG3 thus emerges as a positive regulator of YAP/TAZ-mediated transcription.

To better define the crosstalk between CASA and YAP/TAZ regulation, we adapted a previously established assay for YAP/TAZ activation under tension [21]. In this assay smooth muscle cells are plated on elastomer substrates of varying stiffness, i.e., 0.6 kPa versus 230 kPa, which are coated with the extracellular matrix protein fibronectin (Figure 4G). Depending on substrate stiffness, different levels of tension are generated in cells that contact the substrate through attachment proteins such as integrins [1, 2, 21]. High tension triggered an ~2.5-fold increase in autophagosome number in a manner dependent on BAG3 and SYNPO2 (Figures 4H and 4I). Moreover, autophagy induction was accompanied by increased LC3B lipidation and elevated BAG3 expression (Figure 4J). The findings reveal CASA as a tension-induced autophagy pathway.

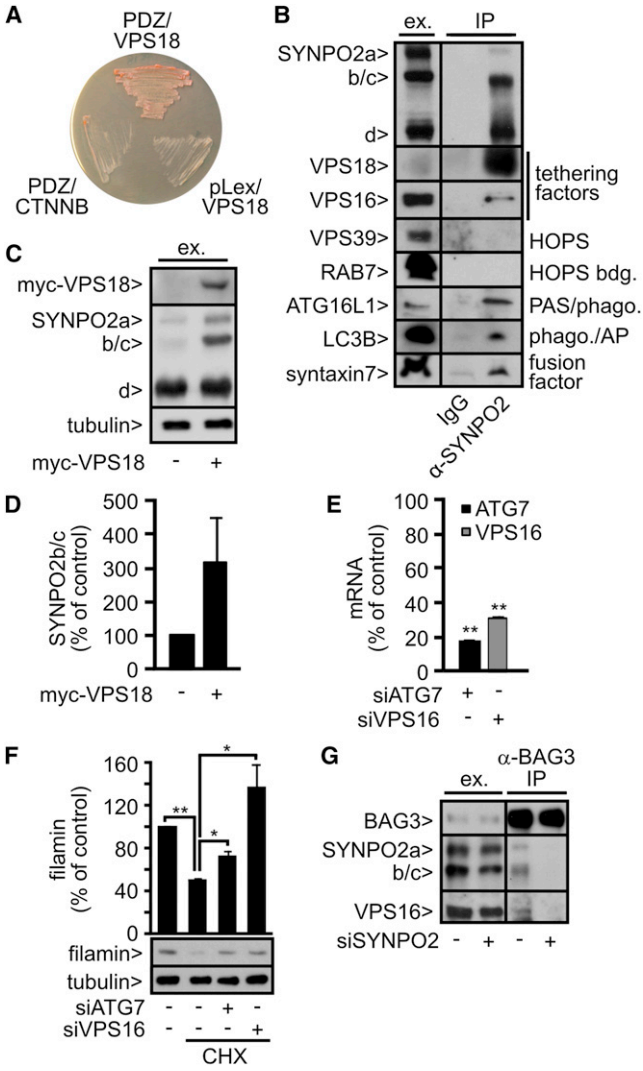

Figure 3. SYNPO2 Links the CASA Machinery to a Membrane-Tethering Complex

(A) The PDZ domain of SYNPO2 (PDZ) interacts with VPS18 in the yeast two-hybrid assay. Control cells carried empty pLex, pAct-*vps18*, and pAct-*ctnnb* (β-catenin), as indicated.

(B) Immunoprecipitation (IP) of endogenous SYNPO2 complexes from A7r5 cells. Indicated proteins were detected with specific antibodies (see Figure 1F for coprecipitation of CASA components). Ex., extract (60 μg of protein); bdg., binding; PAS, preautophagosomal structure; phago., phagophore; AP, autophagosome.

(C) Transient expression of VPS18 for 48 hr stabilizes SYNPO2a to SYNPO2c in A7r5 cells (60 μg of protein per lane).

(D) Quantification of data obtained as described under (C). Mean ± SEM, n = 3.

(E) Quantification of transcripts for ATG7 and VPS16 48 hr after transfection of A7r5 cells with the indicated siRNAs. Transcript levels were compared to levels in cells that received control siRNA (100%). Mean ± SEM, n = 3, **$p < 0.005$.

(F) Filamin levels were determined in A7r5 cells depleted for ATG7 and VPS16 as described under (E). Where indicated, cells were treated with 50 μM cycloheximide (CHX) for 12 hr before lysis to inhibit protein synthesis. Mean ± SEM, n = 3, *$p < 0.05$; **$p < 0.005$.

(G) Immunoprecipitation (IP) of endogenous BAG3 complexes from A7r5 cells. Cells were transfected with control siRNA (−) or siSYNPO2 (+) for 72 hr before immunoprecipitation. Ex., extract; 60 μg of protein per lane.

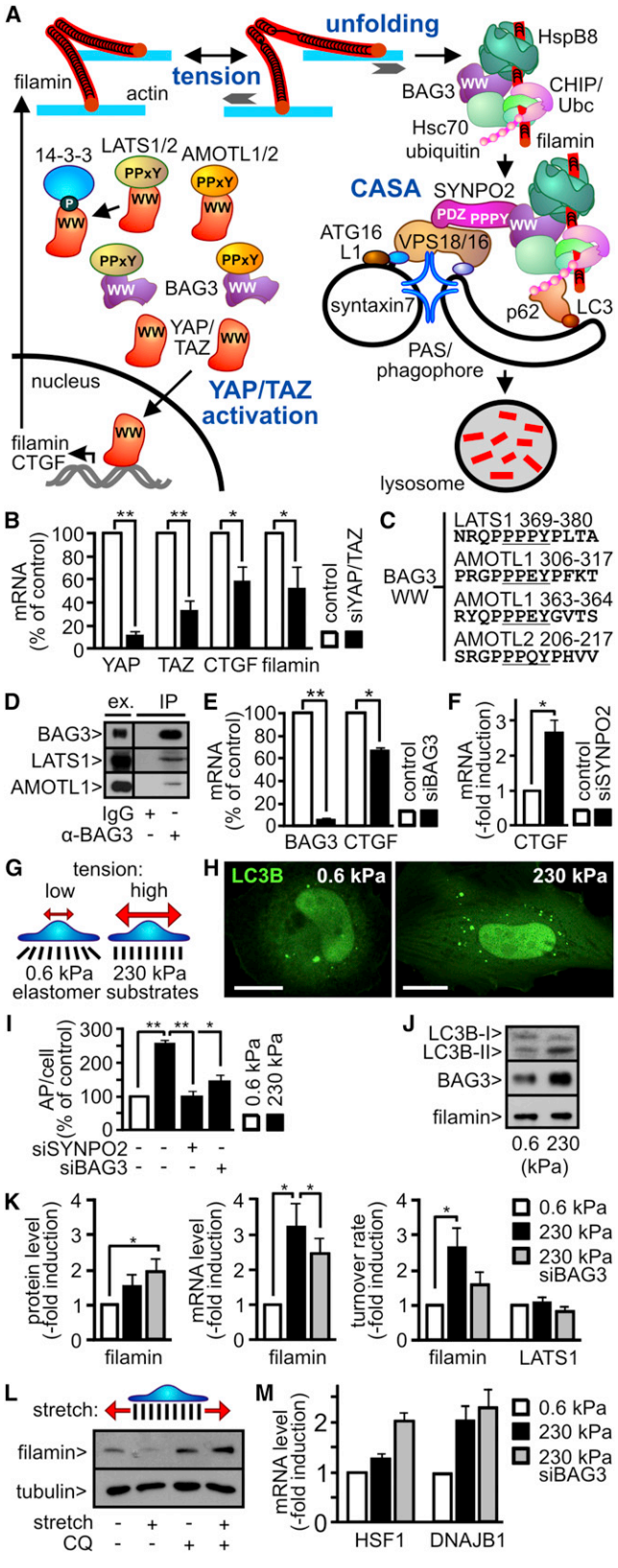

Figure 4. BAG3 Regulates Transcription and Degradation in Response to Mechanical Tension

(A) Schematic representation of BAG3-mediated mechanotransduction. PAS, preautophagosomal structures; Ubc, ubiquitin-conjugating enzyme.

(B) After transfection with control siRNA or cotransfection of siRNAs against *yap* and *taz*, A7r5 cells were allowed to attach for 16 hr in fibronectin-coated cell culture dishes, followed by cell lysis and transcript quantification. Filamin refers to FLNA. Mean ± SEM, n = 3, *p < 0.05; **p < 0.005.

(C) PPxY-containing peptides of YAP/TAZ inhibitors recognized by the BAG3 WW domain in the array screen (see Figure 1A).

(D) Immunoprecipitation (IP) of endogenous BAG3 from A7r5 cells. Indicated components were detected with specific antibodies. Ex., extract; 60 μg of protein.

(E) Transcript quantification for BAG3-depleted cells grown as described under (B). Mean ± SEM, n = 3, *p < 0.05; **p < 0.005.

(F) Transcript quantification for SYNPO2-depleted cells grown as described under (B). Mean ± SEM, n = 3, *p < 0.05; **p < 0.005.

(G) Fibronectin-coated elastomer substrates of different stiffness, i.e., 0.6 kPa versus 230 kPa, were used to induce different amounts of tension in adherent A7r5 smooth muscle cells.

(H) Autophagy was monitored in A7r5 cells, transfected with fluorescently labeled LC3B, and grown under low and high tension for 16 hr. Scale bars represent 20 μm.

(I) Quantification of autophagosomes (AP) in cells grown as described under (H) by automated confocal z stack analysis. Mean ± SEM, n = 3, 20 cells analyzed for each sample in each experiment, *p < 0.05, **p < 0.005.

(J) Immunoblot analysis of untransfected A7r5 cells grown under the same conditions as described under (H).

(K) A7r5 cells were transfected with control siRNA or siBAG3 for 48 hr and afterward plated on fibronectin-coated elastomer substrates for 16 hr, prior to quantification of protein and transcript levels for the indicated components. Turnover rates were calculated by dividing the values obtained for mRNA and protein levels. Mean ± SEM, n = 5, *p < 0.05.

(L) Filamin levels were monitored in A7r5 cells subjected to cyclic stretch for 3 hr. When indicated, the lysosomal proteolysis inhibitor chloroquine (CQ; 100 μM) was added 2 hr before stretching.

(M) A7r5 cells were transfected with control siRNA or siBAG3 for 48 hr and afterward plated on fibronectin-coated elastomer substrates for 16 hr, prior to quantification of transcript levels for the indicated components. Mean ± SEM, n = 4.

See Figures S3 and S4 for related data.

Remarkably, levels of the CASA client filamin did not decline in smooth muscle cells under high tension (Figures 4J and 4K). A concomitant upregulation of filamin transcription may explain this finding, all the more because filamin is a transcriptional target of YAP/TAZ (Figure 4B). Indeed, filamin mRNA level increased ~3-fold under high tension (Figure 4K). Moreover, full induction was dependent on BAG3, consistent with its stimulatory role in YAP/TAZ-mediated transcription. Maintaining filamin levels despite tension-induced autophagic degradation apparently relies on a transcriptional response to provide newly synthesized protein. Correlating transcript and protein levels finally revealed a tension-induced and BAG3-mediated turnover of filamin (Figure 4K). In conclusion, BAG3 acts as a regulator of both transcription and degradation in mechanically strained cells.

When smooth muscle cells were subjected to an acute mechanical insult by short-term cyclic stretching, autophagic degradation of filamin exceeded compensatory synthesis, as is evident from an ~50% decline of filamin protein level under stretch, which was not observed upon autophagy inhibition (Figure 4L).

Smooth muscle cells and nonmuscle cells express a filamin isoform (FLNA) that differs from the striated muscle isoform FLNC [22]. The data obtained here and our previous work on the role of CASA in muscles [5] illustrate that both filamin isoforms are targeted by the BAG3-containing CASA machinery, suggesting a widespread cellular mechanism. Indeed, BAG3 critically regulates the adhesion and motility of diverse cell types [8, 23]. We extended our analysis to immune cells, which rely on tension-regulated adhesion and migration for their recruitment to sites of injury, infection, and inflammation [4].

Inhibition of autophagy strongly impaired the adhesion, spreading, and migration of human Jurkat T lymphoblasts (Figures S3A–S3C) and attenuated the resistance of lymphoblasts and human primary leukocytes to shear stress (Figures S3D and S3E). Moreover, stimulation of adhesion and spreading significantly induced BAG3 expression and filamin turnover in Jurkat cells (Figure S3F). CASA thus emerges as a widely used cellular mechanism for adaptation to mechanical force.

The YAP/TAZ inhibitor LATS1 was not subjected to increased turnover in mechanically strained smooth muscle cells, despite its binding to BAG3 (Figures 4D and 4K). Apparently, BAG3 utilizes its WW domain to either engage in autophagy initiation together with SYNPO2 or to bind YAP/TAZ inhibitors during transcription regulation (Figure 4A). Under low tension, BAG3 levels are low and consequently filamin transcription and degradation are balanced at a low level. Tension induces BAG3 expression (Figure 4J), leading to increased filamin degradation and compensatory upregulation of filamin transcription. Notably, BAG3 is a stress-inducible cochaperone under control of the heat shock transcription factor HSF1 [24]. High tension indeed caused an induction of HSF1 and the HSF1 target gene DNAJB1 in smooth muscle cells (Figure 4M). Moreover, BAG3 depletion, which abrogates the ability to cope with protein damage in mechanically strained cells, further stimulated HSF1 and DNAJB1 expression. Tension-induced unfolding of mechanosensors and cytoskeleton components seems to evoke an adaptation program similar to a heat shock response, involving HSF1 induction, which in turn triggers BAG3 expression and CASA. In this way, autophagic flux through CASA is constantly adjusted to the level of tension within the actin cytoskeleton.

The CASA client filamin is a central mechanosensor [25]. It mediates integrin-actin and actin-actin interactions and thereby senses externally applied force and intracellular tension [22, 25–28]. Filamin is a homodimer consisting of two ~250 kDa rods, each formed by an amino-terminal actin-binding domain followed by 24 immunoglobulin-like (Ig) repeats (Figure S4A). Mechanical unfolding of filamin involves the disruption of interactions between Ig domains 16 through 21 and the loss of secondary structure elements within single Ig domains, which both affect partner protein binding [22, 25, 28, 29]. We mapped the BAG3-binding site in filamin to Ig19-21 (Figures S4A and S4B), which overlapped with the mechanosensitive integrin-binding site [30]. The BAG3 chaperone partners Hsc70 and HspB8 showed only a very weak interaction with Ig19-21 on their own (Figures S4C and S4D). However, in the presence of BAG3, increased amounts of the chaperones were retained on Ig19-21, which in turn also stimulated binding of BAG3 to the domains (Figures S4C–S4E). Cooperative binding of BAG3, Hsc70, and HspB8 to a mechanosensitive region of filamin provides a molecular basis for sensing tension-induced unfolding.

Our data show that BAG3 coordinates tension sensing, autophagosome formation, and transcription regulation and thus acts as a key transducer of mechanical signals in mammalian cells. By targeting filamin, with its multitude of binding partners [22], BAG3 exerts protein quality control at a major mechanosensitive interaction hub. The necessity to induce autophagic degradation at this hub probably arises from structural features of filamin. The large size of the protein combined with the linear arrangement of a large number of individual folding entities, i.e., 24 Ig repeats, might hinder efficient degradation by the proteasome. Still, autophagosome formation at the hub may provide a means for the codegradation and thus coregulation of other hub components.

CASA is induced in adherent cells under tension (see above) and in contracting muscles [5]. The identification of a tension-induced autophagy pathway explains the high reliance on autophagy for the development and maintenance of mechanically strained tissues [31]. Indeed, CASA is required for lung and muscle homeostasis, and its impairment causes muscular dystrophy and cardiomyopathy [5, 32–35]. The observed crosstalk between CASA and YAP/TAZ regulation also appears to be of pathophysiological relevance with regard to tumor formation, known to be affected by mechanical cues [3]. YAP and TAZ, as well as BAG3, are overexpressed in different tumors and display oncogenic activity [7, 23, 36–40]. In contrast, SYNPO2 acts as a tumor suppressor [11]. The opposing roles of these proteins in tumorigenesis can be conclusively explained by the interaction network identified here. Elevated BAG3 expression leads to YAP/TAZ activation, which drives oncogenic transformation, whereas increased SYNPO2 levels would sequester BAG3 to the autophagy machinery, causing YAP/TAZ inactivation and tumor suppression. BAG3-mediated mechanotransduction is apparently intimately linked to tissue homeostasis and growth control in mammals.

Supplemental Information

Supplemental Information includes Supplemental Experimental Procedures and four figures and can be found with this article online at http://dx.doi.org/10.1016/j.cub.2013.01.064.

Acknowledgments

We thank U. Kukulies, K. Himmelberg, and C. Mirschkorsch for technical support, and M. Rusch for mice propagation. We thank G. Dreissen for generating image processing routines and R. Merkel for comments on the manuscript. This work was supported by the DFG (SPP 1580 to A.H. and P.S., BE 4685/1-1 to C.B., FOR 1228 to D.O.F., FOR 1352 to D.O.F. and J.H., DIP 5-1 to J.H., SFB 635 to J.H., VO 885/3-2 to R.V., and SFB 645 to W.K. and J.H.) and by the BMBF (0315501A to B.H.).

Received: August 7, 2012
Revised: December 6, 2012
Accepted: January 29, 2013
Published: February 21, 2013

References

1. Eyckmans, J., Boudou, T., Yu, X., and Chen, C.S. (2011). A hitchhiker's guide to mechanobiology. Dev. Cell *21*, 35–47.
2. Discher, D.E., Janmey, P., and Wang, Y.L. (2005). Tissue cells feel and respond to the stiffness of their substrate. Science *310*, 1139–1143.
3. Hoffman, B.D., Grashoff, C., and Schwartz, M.A. (2011). Dynamic molecular processes mediate cellular mechanotransduction. Nature *475*, 316–323.
4. Alon, R., and Dustin, M.L. (2007). Force as a facilitator of integrin conformational changes during leukocyte arrest on blood vessels and antigen-presenting cells. Immunity *26*, 17–27.
5. Arndt, V., Dick, N., Tawo, R., Dreiseidler, M., Wenzel, D., Hesse, M., Fürst, D.O., Saftig, P., Saint, R., Fleischmann, B.K., et al. (2010). Chaperone-assisted selective autophagy is essential for muscle maintenance. Curr. Biol. *20*, 143–148.
6. Sudol, M., and Harvey, K.F. (2010). Modularity in the Hippo signaling pathway. Trends Biochem. Sci. *35*, 627–633.
7. Salah, Z., Alian, A., and Aqeilan, R.I. (2012). WW domain-containing proteins: retrospectives and the future. Front. Biosci. *17*, 331–348.
8. Iwasaki, M., Tanaka, R., Hishiya, A., Homma, S., Reed, J.C., and Takayama, S. (2010). BAG3 directly associates with guanine nucleotide exchange factor of Rap1, PDZGEF2, and regulates cell adhesion. Biochem. Biophys. Res. Commun. *400*, 413–418.

9. Sanchez-Carbayo, M., Schwarz, K., Charytonowicz, E., Cordon-Cardo, C., and Mundel, P. (2003). Tumor suppressor role for myopodin in bladder cancer: loss of nuclear expression of myopodin is cell-cycle dependent and predicts clinical outcome. Oncogene *22*, 5298–5305.
10. Linnemann, A., van der Ven, P.F., Vakeel, P., Albinus, B., Simonis, D., Bendas, G., Schenk, J.A., Micheel, B., Kley, R.A., and Fürst, D.O. (2010). The sarcomeric Z-disc component myopodin is a multiadapter protein that interacts with filamin and alpha-actinin. Eur. J. Cell Biol. *89*, 681–692.
11. Yu, Y.P., and Luo, J.H. (2011). Phosphorylation and interaction of myopodin by integrin-link kinase lead to suppression of cell growth and motility in prostate cancer cells. Oncogene *30*, 4855–4863.
12. Pandey, U.B., Nie, Z., Batlevi, Y., McCray, B.A., Ritson, G.P., Nedelsky, N.B., Schwartz, S.L., DiProspero, N.A., Knight, M.A., Schuldiner, O., et al. (2007). HDAC6 rescues neurodegeneration and provides an essential link between autophagy and the UPS. Nature *447*, 859–863.
13. Tanaka, Y., Guhde, G., Suter, A., Eskelinen, E.L., Hartmann, D., Lüllmann-Rauch, R., Janssen, P.M., Blanz, J., von Figura, K., and Saftig, P. (2000). Accumulation of autophagic vacuoles and cardiomyopathy in LAMP-2-deficient mice. Nature *406*, 902–906.
14. Rubinsztein, D.C., Shpilka, T., and Elazar, Z. (2012). Mechanisms of autophagosome biogenesis. Curr. Biol. *22*, R29–R34.
15. Epp, N., Rethmeier, R., Krämer, L., and Ungermann, C. (2011). Membrane dynamics and fusion at late endosomes and vacuoles—Rab regulation, multisubunit tethering complexes and SNAREs. Eur. J. Cell Biol. *90*, 779–785.
16. Wickner, W. (2010). Membrane fusion: five lipids, four SNAREs, three chaperones, two nucleotides, and a Rab, all dancing in a ring on yeast vacuoles. Annu. Rev. Cell Dev. Biol. *26*, 115–136.
17. Bröcker, C., Kuhlee, A., Gatsogiannis, C., Balderhaar, H.J., Hönscher, C., Engelbrecht-Vandré, S., Ungermann, C., and Raunser, S. (2012). Molecular architecture of the multisubunit homotypic fusion and vacuole protein sorting (HOPS) tethering complex. Proc. Natl. Acad. Sci. USA *109*, 1991–1996.
18. Moreau, K., Ravikumar, B., Renna, M., Puri, C., and Rubinsztein, D.C. (2011). Autophagosome precursor maturation requires homotypic fusion. Cell *146*, 303–317.
19. Xu, L., Sowa, M.E., Chen, J., Li, X., Gygi, S.P., and Harper, J.W. (2008). An FTS/Hook/p107(FHIP) complex interacts with and promotes endosomal clustering by the homotypic vacuolar protein sorting complex. Mol. Biol. Cell *19*, 5059–5071.
20. Arlt, H., Perz, A., and Ungermann, C. (2011). An overexpression screen in Saccharomyces cerevisiae identifies novel genes that affect endocytic protein trafficking. Traffic *12*, 1592–1603.
21. Dupont, S., Morsut, L., Aragona, M., Enzo, E., Giulitti, S., Cordenonsi, M., Zanconato, F., Le Digabel, J., Forcato, M., Bicciato, S., et al. (2011). Role of YAP/TAZ in mechanotransduction. Nature *474*, 179–183.
22. Nakamura, F., Stossel, T.P., and Hartwig, J.H. (2011). The filamins: organizers of cell structure and function. Cell Adhes. Migr. *5*, 160–169.
23. Iwasaki, M., Homma, S., Hishiya, A., Dolezal, S.J., Reed, J.C., and Takayama, S. (2007). BAG3 regulates motility and adhesion of epithelial cancer cells. Cancer Res. *67*, 10252–10259.
24. Franceschelli, S., Rosati, A., Lerose, R., De Nicola, S., Turco, M.C., and Pascale, M. (2008). Bag3 gene expression is regulated by heat shock factor 1. J. Cell. Physiol. *215*, 575–577.
25. Ehrlicher, A.J., Nakamura, F., Hartwig, J.H., Weitz, D.A., and Stossel, T.P. (2011). Mechanical strain in actin networks regulates FilGAP and integrin binding to filamin A. Nature *478*, 260–263.
26. Engler, A.J., Carag-Krieger, C., Johnson, C.P., Raab, M., Tang, H.Y., Speicher, D.W., Sanger, J.W., Sanger, J.M., and Discher, D.E. (2008). Embryonic cardiomyocytes beat best on a matrix with heart-like elasticity: scar-like rigidity inhibits beating. J. Cell Sci. *121*, 3794–3802.
27. Johnson, C.P., Tang, H.Y., Carag, C., Speicher, D.W., and Discher, D.E. (2007). Forced unfolding of proteins within cells. Science *317*, 663–666.
28. Rognoni, L., Stigler, J., Pelz, B., Ylänne, J., and Rief, M. (2012). Dynamic force sensing of filamin revealed in single-molecule experiments. Proc. Natl. Acad. Sci. USA *109*, 19679–19684.
29. Chen, H., Zhu, X., Cong, P., Sheetz, M.P., Nakamura, F., and Yan, J. (2011). Differential mechanical stability of filamin A rod segments. Biophys. J. *101*, 1231–1237.
30. Lad, Y., Kiema, T., Jiang, P., Pentikäinen, O.T., Coles, C.H., Campbell, I.D., Calderwood, D.A., and Ylänne, J. (2007). Structure of three tandem filamin domains reveals auto-inhibition of ligand binding. EMBO J. *26*, 3993–4004.
31. Mizushima, N., and Komatsu, M. (2011). Autophagy: renovation of cells and tissues. Cell *147*, 728–741.
32. Homma, S., Iwasaki, M., Shelton, G.D., Engvall, E., Reed, J.C., and Takayama, S. (2006). BAG3 deficiency results in fulminant myopathy and early lethality. Am. J. Pathol. *169*, 761–773.
33. Selcen, D., Muntoni, F., Burton, B.K., Pegoraro, E., Sewry, C., Bite, A.V., and Engel, A.G. (2009). Mutation in BAG3 causes severe dominant childhood muscular dystrophy. Ann. Neurol. *65*, 83–89.
34. Arimura, T., Ishikawa, T., Nunoda, S., Kawai, S., and Kimura, A. (2011). Dilated cardiomyopathy-associated BAG3 mutations impair Z-disc assembly and enhance sensitivity to apoptosis in cardiomyocytes. Hum. Mutat. *32*, 1481–1491.
35. Sarparanta, J., Jonson, P.H., Golzio, C., Sandell, S., Luque, H., Screen, M., McDonald, K., Stajich, J.M., Mahjneh, I., Vihola, A., et al. (2012). Mutations affecting the cytoplasmic functions of the co-chaperone DNAJB6 cause limb-girdle muscular dystrophy. Nat Genet. *44*, 450–455.
36. Festa, M., Del Valle, L., Khalili, K., Franco, R., Scognamiglio, G., Graziano, V., De Laurenzi, V., Turco, M.C., and Rosati, A. (2011). BAG3 protein is overexpressed in human glioblastoma and is a potential target for therapy. Am. J. Pathol. *178*, 2504–2512.
37. Suzuki, M., Iwasaki, M., Sugio, A., Hishiya, A., Tanaka, R., Endo, T., Takayama, S., and Saito, T. (2011). BAG3 (BCL2-associated athanogene 3) interacts with MMP-2 to positively regulate invasion by ovarian carcinoma cells. Cancer Lett. *303*, 65–71.
38. Li, N., Du, Z.X., Zong, Z.H., Liu, B.Q., Li, C., Zhang, Q., and Wang, H.Q. (2012). PKCδ-mediated phosphorylation of BAG3 at Ser187 site induces epithelial-mesenchymal transition and enhances invasiveness in thyroid cancer FRO cells. Oncogene. Published online October 29, 2012. http://dx.doi.org/10.1038/onc.2012.466.
39. Cordenonsi, M., Zanconato, F., Azzolin, L., Forcato, M., Rosato, A., Frasson, C., Inui, M., Montagner, M., Parenti, A.R., Poletti, A., et al. (2011). The Hippo transducer TAZ confers cancer stem cell-related traits on breast cancer cells. Cell *147*, 759–772.
40. Zhao, B., Li, L., Lei, Q., and Guan, K.L. (2010). The Hippo-YAP pathway in organ size control and tumorigenesis: an updated version. Genes Dev. *24*, 862–874.